JOURNAL OF CATALYSIS **178,** 264–274 (1998)
ARTICLE NO. CA982159

Ortho-Selective Methylation of Phenol Catalyzed by CeO_2-MgO Prepared by Citrate Process

Satoshi Sato,[1] Kaoru Koizumi, and Fumio Nozaki

Department of Applied Chemistry, Faculty of Engineering, Chiba University, Yayoi, Inage, Chiba 263-8522, Japan

Received November 11, 1997; revised May 4, 1998; accepted May 18, 1998

Vapor-phase alkylation of phenol with methanol was investigated over CeO_2-MgO catalysts prepared utilizing a molten mixture of the corresponding nitrates and citric acid. The CeO_2-MgO had attractive catalytic performance without decay of activities at the temperature range between 450 and 550°C, and it had excellent selectivities to the sum of *o*-cresol and 2,6-xylenol higher than 98%. The CeO_2-MgO catalysts were found to be mixtures of MgO and an interstitial solid solution of $Mg_xCe_{1-x/2}O_2$ as a result of XRD measurement. It is confirmed that citric acid used in the preparation heightens the dispersion of the solid solution in the MgO matrix. The pure CeO_2, which also exhibited efficient ortho-selectivity, had only weak basic sites in the TPD experiment of adsorbed CO_2, while the pure MgO with strong basicity showed very low reaction rate in the methylation. The solid solution of $Mg_xCe_{1-x/2}O_2$ in the CeO_2-MgO catalyst probably provides active centers for the methylation of phenol. In the results of methanol decomposition, methanol was converted into CO, CO_2, and CH_4 over the CeO_2-MgO catalysts, without producing dimethyl ether. The reaction mechanism of the ortho-methylation over the CeO_2-MgO catalyst is speculated: the ortho position of phenol adsorbed perpendicularly on weak basic sites on the $Mg_xCe_{1-x/2}O_2$ solid solution is selectively alkylated by methanol which is possibly activated in the form of formyl or hydroxy methyl group rather than methyl cation.

Key Words: **alkylation; phenol; methanol; CeO_2-MgO; base; citric acid.**

INTRODUCTION

Alkylated phenols such as *o*-cresol and 2,6-xylenol are important chemicals as intermediates in agrochemical and polymer industries. Cresols, xylenols, and other methylated products are produced by alkylation of phenol with methanol. Vapor-phase methylation of phenol has been investigated over various metal oxides such as MgO (1–4), Mn_3O_4 (5), and Al_2O_3 (6–8), acidic zeolites such as H-ZSM5 (6, 7, 9, 10), and HY (6, 7, 10), and other mixed metal oxides such as MgO-based (1, 3), Fe_2O_3-based (11–15), V_2O_5-based oxides (15–18), and Al-containing hydrotalcites (19–21). The mixed metal oxides with acid–base properties (11–21), as well as the basic MgO (1–4) are selective catalysts for the ortho-methylation, because the reactant phenol is perpendicularly adsorbed on the surface. The acidic catalysts such as alumina and zeolites (6–10), however, catalyze both the ring-alkylation and oxygen-alkylation of phenol adsorbed horizontally on the surface of the catalysts (8). In a preliminary examination for the methylation of phenol over various oxides of rare earth metals, we reported that only CeO_2 had efficient catalytic activity for the ortho-methylation of phenol without decay (4).

On the other hand, citric acid is utilized for preparing ceramic powders with high crystallinity (22). The technique is known as an amorphous citrate process and is also applied to the preparation of catalysts such as perovskite-type (23–26) and spinel-type composite oxides (27–30), as well as porous magnesium oxide (31). In our recent work, Ni-MgO catalysts which were prepared using a molten mixture of nickel nitrate, magnesium nitrate, and citric acid has been found to have high nickel metal surface areas and efficient catalytic activities for the hydrogenolysis (32) and hydrogenation (33, 34). It is confirmed that citric acid used in the preparation improved the homogeneity of the components.

In this paper, we describe the characteristics of CeO_2-MgO catalysts prepared by the citrate process. In addition, we examine the relation between the catalytic efficiency and the basicity of the CeO_2-MgO catalysts, which exhibit excellent catalytic performance for the ortho-selective methylation of phenol.

EXPERIMENTAL

Catalyst Preparation

All reagents were supplied by Wako Chemical Ltd., Japan. Each CeO_2-MgO sample with different contents was prepared by using cerium (III) nitrate hexahydrate, magnesium nitrate hexahydrate, and citric acid monohydrate. The procedure is essentially the same method as for an amorphous citrate process (22), where water is used as a solvent. A mixture of cerium (III) nitrate and magnesium nitrate with a desired molar ratio was melted with citric acid, which

[1] Corresponding author. E-mail: satoshi@planet.tc.chiba-u.ac.jp.

0021-9517/98 $25.00

was equimolar to the sum of cerium and magnesium ions, in a flask (300 cm^3 for the total metal ions of about 70 mmol) without using solvents at 70°C (31–34). Then, the molten mixture was evacuated in a rotary evaporator under a pressure of 0.7 kPa at 70°C. The molten mixture was gradually solidified, and then expanded. After the resulting solid had been heated in air at 170°C for 2 h, it was calcined in air at 550°C for 2 h to give a CeO_2-MgO sample.

Catalytic Reaction

The alkylation of phenol with methanol was carried out in a usual fixed-bed flow reactor under atmospheric pressure of helium at a temperature range between 450 and 600°C. Prior to the reaction, a catalyst sample (0.1 g) was preheated in a glass tube reactor at the same temperature as the reaction temperature for 1 h. A mixture of phenol and methanol with a molar ratio of 1 : 4 was fed into the reactor at a total flow rate of 25 mmol h^{-1}, together with helium flow (50 mmol h^{-1}). An effluent was collected in an ice trap and was analyzed by FID-GC with a packed column of Silicon OV-17 (2 m) at temperatures controlled from 120 to 220°C at a heating rate of 10 K min^{-1}. The catalytic activity was evaluated in terms of an average conversion of phenol for every hour. The reaction rate was calculated at 450°C from a slope of a W/F-conversion curve, where W and F were the catalyst weight (g) and the flow rate of phenol (5 mmol h^{-1}), respectively. The conversion of phenol is defined as a fraction of reacted phenol, and the ortho-selectivity is as a sum of the selectivities to *o*-cresol and 2,6-xylenol.

Methanol decomposition was also performed in the fixed bed flow reactor under atmospheric pressure of helium at the temperature range between 450 and 600°C. A catalyst sample (0.15 g) was preheated in the glass tube reactor at the same temperature as the reaction temperature for 1 h, prior to the reaction. Methanol was fed into the reactor at the flow rate 128 mmol h^{-1} with helium carrier (88 mmol h^{-1}). Reaction products were detected by TCD detector after being separated by on-line GC with packed columns of PEG 1500 (2 m) and activated carbon (2 m) at 40°C; after the reactant methanol had been separated from the reaction products with the PEG 1500 column, the reaction products such as CO, CO_2, and CH_4 were separated with the activated carbon column.

Characterization

The temperature-programmed desorption (TPD) of adsorbed CO_2 was measured by neutralization titration using an electric conductivity cell immersed in an aqueous solution, as has been described in the TPD experiment of adsorbed NH_3 (35–37). A sample (20 mg) held with quartz wool in a quartz tube was preheated in nitrogen flow at 500°C for 1 h. Carbon dioxide (1.0 mmol) was charged into the quartz tube by using a syringe. After the tube had been stored in a desicator at 25°C for 72 h, the tube was attached to the TPD line. After physisorbed CO_2 had been purged at 25°C in a nitrogen flow, the TPD measurement was started from 25 to 800°C at a heating rate of 10 K min^{-1} under a nitrogen flow of 37 mmol h^{-1}. The desorbed CO_2, together with nitrogen, was bubbled into an electric conductivity cell containing 2.0 mmol dm^{-3} of a sodium hydroxide solution (50.0 g). The amount of desorbed CO_2 was monitored by the change in the conductivity of the solution. A cumulative amount of desorbed CO_2 was obtained as a function of the desorption temperature and then differentiated to give a TPD profile as a base strength distribution.

The TPD of adsorbed NH_3 was also examined by neutralization titration in a diluted sulfuric acid solution, according to the procedure reported elsewhere (35–37). After the sample had been evacuated at 500°C under a reduced pressure of 1.3 Pa, NH_3 vapor was introduced at 13 kPa at 25°C.

A total surface area of the sample was calculated by the BET method using nitrogen isotherm at −196°C. XRD spectra of the samples were recorded by M18XHF (Mac Science).

RESULTS

Preliminarily, various metal oxides were introduced into MgO as second components of MgO-based mixed oxides in the citrate process, and the catalytic activities of the MgO-based mixed oxide systems were examined. Table 1 summarizes the catalytic results at a reaction temperature of 500°C. An average conversion between 1 and 2 h is listed as an initial catalytic activity, and an average conversion between 4 and 5 h is also shown in the parenthesis. The initial catalytic activities of composite systems of Na, B, Tl, Zr, Ce, and U with MgO surpassed that of the pure MgO. In particular, the addition of U and Ce into MgO greatly enhanced the initial catalytic activities. The composite systems of Na, B, Tl, Zr, and U with MgO, however, were deactivated with process time, except for CeO_2-MgO system. The addition of other metals such as Li, K, Cs, Ca, Sr, Ba, Al, La, Pr, Sm, Dy, and Yb were ineffective for the enhancement of the catalytic activity of MgO. Among the composite systems we tested, only the CeO_2-MgO system exhibited an efficient catalytic activity without decay. All of the catalysts, except for Cs, had the ortho-selectivities, which is a sum of the selectivities to *o*-cresol and 2,6-xylenol, higher than 94%.

Figure 1 shows changes in the catalytic activities of the CeO_2-MgO with process time at 500°C, together with the results of pure CeO_2 and MgO, which were prepared from the melt of the individual nitrate and citric acid. As has been preliminarily reported (4), the catalytic activity of the pure MgO decreased with process time (curve a in Fig. 1). The pure CeO_2 catalyst, however, showed a stable activity with a gradual increase in the initial reaction period for 2 h (curve

TABLE 1

Catalytic Properties of Various MgO-Based Mixed Oxide Systems

Second catalyst component[a]	Conversion of phenol[b]/%	Selectivity[b]/%	
		o-Cresol	2,6-Xylenol
None	11.8 (10.3)	93.6	5.0
Li	12.8 (11.9)	93.1	5.4
Na	17.3 (9.9)	92.7	4.7
K	7.7 (4.9)	91.1	3.3
Cs	11.4 (6.2)	61.1	1.7
Ca	10.2 (9.8)	94.0	4.1
Sr	10.4 (10.0)	92.3	5.7
Ba	10.1 (7.8)	92.6	4.0
B	20.4 (14.4)	87.9	9.7
Al	12.4 (10.8)	92.9	4.8
Tl	15.9 (9.9)	91.6	6.8
Zr	15.4 (11.5)	87.3	8.3
La	10.3 (10.2)	92.5	3.5
Ce[c]	32.2 (32.6)	90.0	8.6
Pr	9.7 (8.6)	93.7	3.5
Sm	11.2 (9.6)	93.2	3.7
Dy	10.4 (8.6)	91.8	3.9
Yb	9.7 (8.3)	92.5	4.4
U	40.9 (19.9)	78.9	17.6

[a] Samples were prepared by the citrate process, the second components with the metal content of 0.44 mmol based on MgO of 1.0 g were introduced using the metal nitrate (except for cesium carbonate, zirconyl nitrate, and uranyl acetate) into the system.

[b] Reacted at 500°C, catalyst 0.10 g, average conversion between 1 and 2 h, average conversion between 4 and 5 h in the parenthesis, other products are anisole, *p*-cresol, 2,4-xylenol, and 2,4,6-trimethylphenol.

[c] The CeO_2 content corresponds to 1.8 mol%.

c). For CeO_2(11.2 mol%)-MgO prepared by the citrate process (curve b), the conversion level was higher than that of the pure MgO, and no decay in the catalytic activities was observed as well as in the pure CeO_2. The conversion level of the CeO_2-MgO prepared by impregnation was equal to that of the pure CeO_2 (curve d). The catalyst shown in Fig. 1 had ortho-selectivities higher than 98%.

Figures 2, 3, and 4 exhibit the changes in the phenol conversion with process time at several reaction temperatures, for the pure MgO, the CeO_2(11.2 mol%)-MgO, and the pure CeO_2, respectively. Although the pure MgO showed ortho-selectivities higher than 98%, it had a slight decay in the phenol conversion at temperatures up to 550°C (Fig. 2). On the other hand, the CeO_2-MgO (Fig. 3) and the pure CeO_2 (Fig. 4) showed stable catalytic activities at the temperatures, after the induction periods for 3 h. In contrast to that the phenol conversion greatly increased at reaction temperatures between 500 and 550°C over the pure MgO, it greatly increased between 450 and 500°C over the CeO_2-MgO. Neither change in the color nor in the sample weight of the used CeO_2 catalyst was observed at temperatures lower than 500°C. In contrast, for the used catalysts, the CeO_2-MgO and the pure MgO changed color into gray or brown, while no change in the sample weight was observed

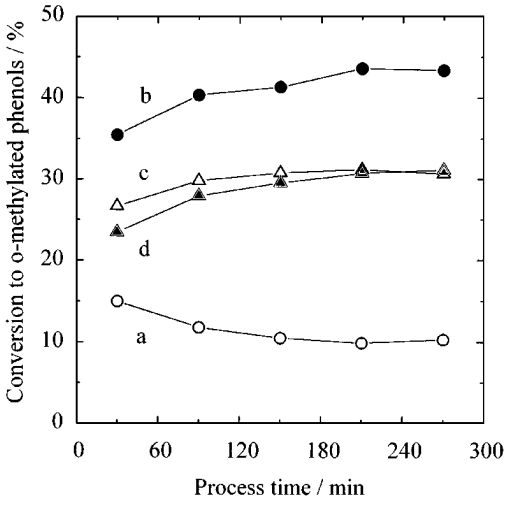

FIG. 1. Comparison of catalytic activities among CeO_2-MgO at a reaction temperature of 500°C: (a) MgO; (b) CeO_2(11.2 mol%)-MgO; (c) CeO_2 prepared by this method; (d) CeO_2(11.2 mol%)-MgO prepared by impregnation.

after the methylation at temperatures lower than 550°C. We did not always monitor the conversion of methanol during the methylation. In a case of the CeO_2-MgO, small amounts of CO and CH_4 were detected at 500°C.

For every catalyst we tested at 600°C (curves d in Figs. 2–4), however, the phenol conversion decreased steeply with process time, and lost its activity by 4 h. In addition, the color of the recovered catalysts was black after use for the methylation at 600°C, and the weight increase of the used catalysts were about 4, 9, and 13% for the CeO_2, the CeO_2-MgO, and the MgO, respectively. Furthermore, in the methylation at 600°C over the CeO_2 and the CeO_2-MgO catalysts, methanol was not recovered, and CO and CH_4 were detected.

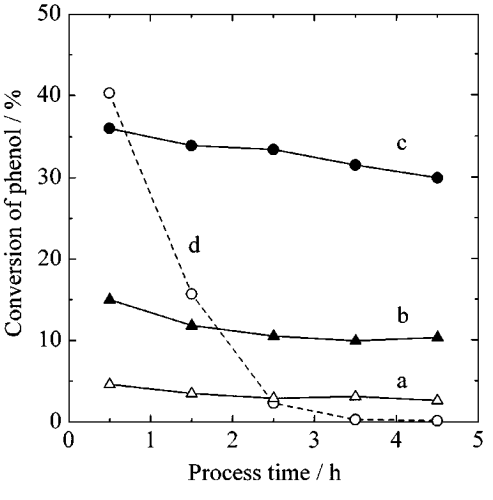

FIG. 2. Variations in catalytic activities with process time of MgO: (a) reacted at 450°C; (b) 500°C; (c) 550°C; (d) 600°C.

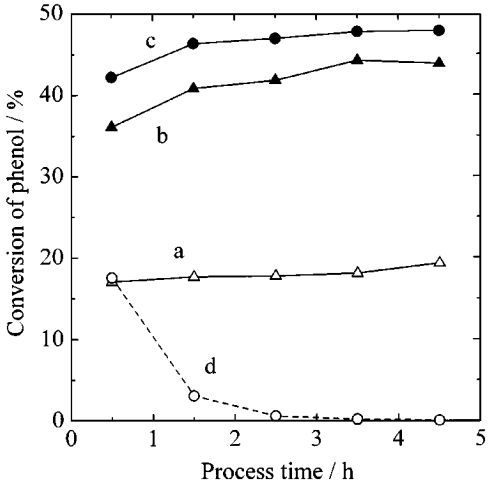

FIG. 3. Variations in catalytic activities with process time of CeO_2-MgO: (a) reacted at 450°C; (b) 500°C; (c) 550°C; (d) 600°C.

Because the consumption of methanol was not calculated during the methylation, the methanol decomposition was tested over the catalysts without phenol. The results are summarized in Table 2. Methanol was completely decomposed into CO, CO_2, and CH_4 at temperatures higher than 550°C over the pure CeO_2 and the CeO_2-MgO, without forming dimethyl ether. Even at reaction temperature as low as 450°C, methanol was decomposed. Over the pure MgO, however, it was decomposed into CO without forming CH_4 and CO_2, in addition to the low conversions of methanol. In the methanol decomposition, no catalytic decay was observed even at 600°C.

Table 3 summarizes the catalytic results, average conversions between 2 and 5 h, of various CeO_2-MgO catalysts at 500°C. In the CeO_2-MgO catalysts prepared by this method, the average conversion at 500°C maximized at the CeO_2 content of 11.2 mol%. The reaction rate based on the sample weight at 450°C was also maximized at the CeO_2 content of 11.2 mol%. Although the selectivity to *o*-cresol decreased with increasing the phenol conversion, the ortho-selectivity to the total of *o*-cresol and 2,6-xylenol exceeded 98% regardless of the CeO_2 content. Another product was anisole (methoxybenzene) with the selectivity less than 1.0%, and trace residuals were *p*-cresol, 2,4-xylenol, and 2,4,6-trimethylphenol. For other reference catalysts as CeO_2-SiO_2 and CeO_2-Al_2O_3, anisole selectivities were higher than 10%, in addition to the low phenol conversions.

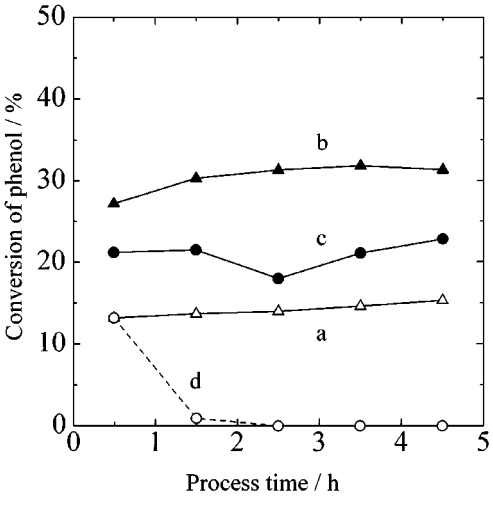

FIG. 4. Variations in catalytic activities with process time of CeO_2: (a) reacted at 450°C; (b) 500°C; (c) 550°C; (d) 600°C.

TABLE 2

Catalytic Activities of Methanol Decomposition over CeO_2[a]

Catalyst	Temperature °C	Conversion of methanol/%	Product distribution/%		
			CO	CH_4	CO_2
MgO	450	1	100	0	0
	500	2	100	0	0
	550	14	100	0	0
	600	35	100	0	0
CeO_2-MgO[b]	450	6	75	25	0
	500	32	59	38	3
	550	100	70	25	5
	600	100	74	21	5
CeO_2	450	10	65	35	0
	500	51	52	44	2
	550	100	58	36	6
	600	100	61	31	8

[a] Average conversion between 1 and 2 h at the prescribed temperature, catalyst 0.15 g, methanol flow rate 128 mmol h^{-1}, carrier helium flow rate 88 mmol h^{-1}.

[b] The CeO_2 content is 11.2 mol%.

Table 4 shows the catalytic results of anisole transformation at 500°C, instead of the reaction of phenol and methanol. Typical samples of MgO, CeO_2-MgO, and CeO_2 preferentially catalyzed the decomposition of anisole into benzene and phenol. Although a small amount of *o*-cresol was produced over the pure MgO, the CeO_2-MgO and the pure CeO_2 had no catalytic activity for the transformation of anisole into *o*-cresol.

Figure 5 illustrates TPD spectra of substrates adsorbed on several catalysts used for the methylation at 500°C for 5 h. Because the TPD detector we used is not responsive to neutral molecules such as methanol and anisole (35, 36), the desorption signals in Fig. 5 are attributed to acidic substrates such as phenol and CO_2. Most of the acidic substrates desorbed from MgO were observed at temperatures higher than 400°C (curve a). In contrast, the acidic substrates adsorbed on the CeO_2(11.2 mol%)-MgO and the pure CeO_2 were desorbed at temperatures lower than 550°C; the peak tops were located at around 300°C (curves b and c).

We performed the TPD experiment using NH_3 and CO_2 as adsorbates in order to estimate the acidity and the

TABLE 3

Catalytic Properties of Various Catalysts

Catalyst	CeO_2 content /mol% (wt%)	Conversion of phenol[a]/%	Selectivity to[a]/%		Reaction rate[b]	
			o-Cresol	2,6-Xylenol	/mmolh^{-1}g^{-1}	/mmolh^{-1}m^{-2}
MgO[c]	0	10.7	94.5	3.7	2.9	0.03
CeO_2-MgO[c]	1.8 (7.3)	32.7	89.9	8.6	6.6	0.07
CeO_2-MgO[c]	3.8 (14.4)	32.9	87.0	11.5	12.3	0.11
CeO_2-MgO[c]	11.2 (35.0)	43.3	84.9	13.5	14.9	0.13
CeO_2-MgO[c]	22.3 (55.1)	41.7	86.8	11.6	12.2	0.12
CeO_2-MgO[c]	40.2 (74.2)	35.7	89.9	8.8	6.4	0.13
CeO_2-MgO[c]	72.1 (91.2)	32.9	90.6	8.0	3.8	0.16
CeO_2[c]	100	31.5	91.8	6.6	9.2	0.21
CeO_2[d]	100	32.1[h]	90.1	8.2	—	—
CeO_2[e]	100	27.4[h]	92.3	6.6	—	—
CeO_2[f]	100	22.4[h]	93.4	5.2	—	—
CeO_2-MgO[g]	1.8 (7.3)	21.5	92.7	5.9	—	—
CeO_2-MgO[g]	3.8 (14.4)	28.6	91.0	8.0	3.9	0.09
CeO_2-MgO[g]	11.2 (35.0)	30.7	90.3	8.9	3.8	0.10
CeO_2-SiO_2[g]	8.0 (27.1)	4.4	79.3	3.9	—	—
CeO_2-Al_2O_3[c]	50 (81.0)	18.2	72.4	10.5	—	—

[a] Reacted at 500°C, catalyst 0.10 g, average conversion between 2 and 5 h.
[b] Reacted at 450°C.
[c] Prepared by this method.
[d] Prepared by thermal decomposition of $Ce(NO_3)_3 \cdot 6H_2O$.
[e] Prepared by thermal decomposition of $Ce_2(CO_3)_3 \cdot 8H_2O$.
[f] Prepared by thermal decomposition of $Ce_2(C_2O_4)_3 \cdot 9H_2O$.
[g] Prepared by impregnation.
[h] The data were referenced in Ref. 4.

basicity of the catalysts, respectively. No NH_3 adsorption was observed at 25°C in the TPD experiment of adsorbed NH_3 for all of the CeO_2-MgO catalysts we examined. Figure 6 depicts TPD spectra of CO_2 adsorbed on several catalysts. CO_2 was desorbed from the catalysts at temperatures lower than 500°C. The pure MgO had large desorption peaks at around 120 and 300°C (curve a). An addition of CeO_2 (11.2 mol%) into MgO decreased the peak at 300°C, and increased the peak at 120°C (curve b). Further addition of CeO_2 (40.2 mol%) into MgO decreased the total amount of desorbed CO_2 (curve c). The pure CeO_2, however, had only a small CO_2 desorption peak at 120°C (curve d).

TABLE 4

Catalytic Activities of Anisole Conversion Reaction[a]

Catalyst[b]	Conversion of anisole/%	Selectivity to /%		
		Benzene	Phenol	*o*-Cresol
MgO	12.4	26.8	69.3	4.0
CeO_2-MgO[c]	9.9	27.2	72.8	0
CeO_2	10.1	27.4	72.6	0

[a] Average conversion between 1 and 2 h at 500°C, catalyst 0.10 g, anisole flow rate 12 mmol h^{-1}, carrier helium flow rate 50 mmol h^{-1}.
[b] Prepared by this method.
[c] The CeO_2 content is 11.2 mol%.

Table 5 is a summary of the total number of basic sites measured by the total amount of desorbed CO_2 in the TPD, together with the data of specific surface areas of the catalysts.

Figure 7 illustrates a TPD spectrum of CO_2 adsorbed on the pure MgO and its deconvolution. The TPD spectrum

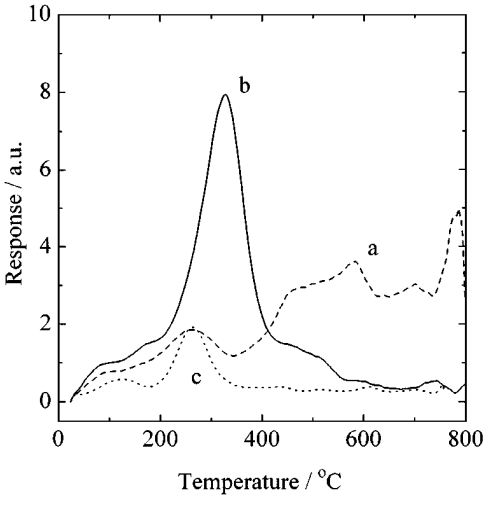

FIG. 5. TPD spectra of substrates adsorbed on the catalysts used for the reaction at 500°C: (a) MgO; (b) CeO_2(11.2 mol%)-MgO; (c) CeO_2 prepared by this method.

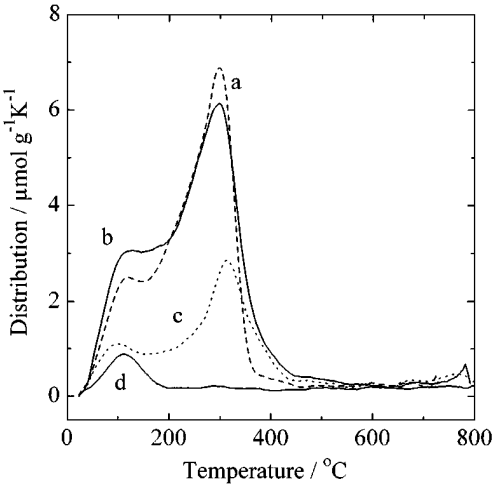

FIG. 6. TPD spectra of CO_2 adsorbed on the catalysts: (a) MgO; (b) CeO_2(11.2 mol%)-MgO; (c) CeO_2(40.2 mol%)-MgO; (d) CeO_2 prepared by this method.

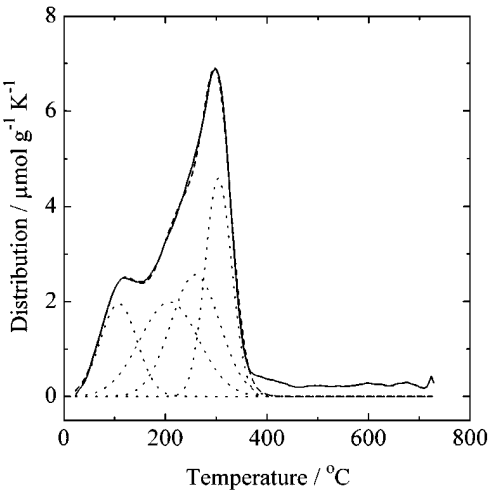

FIG. 7. TPD profile of CO_2 adsorbed on MgO and its deconvolution: solid curve is for experimental; dotted curves are for its deconvolution; and broken curve is for its convolution.

was able to be deconvoluted into four Gausian peaks (dotted curves), and the convolution (broken curve) had a good fit to the experimental spectrum (solid curve). The TPD spectra of CO_2 adsorbed on the catalysts (Fig. 6) were also deconvoluted into four Gausian peaks as the example of MgO shown in Fig. 7, and the convolution curves are well fitted to the experimental spectra. Since only weak basic sites are observed on the pure CeO_2 which is active for the ortho-methylation, strong basic sites must be irrelevant to the catalytic reaction at temperatures lower than 500°C. Then, a peak whose top was at temperatures lower than 150°C was obtained as weak basic sites by deconvoluting the TPD spectrum (the fourth column of Table 5). The number of weak basic sites was maximized at the CeO_2 content of 11.2 mol%. We calculated the density of weak basic sites using values of the number of weak basic sites and the specific surface areas (the last column of Table 5), whereas the density of total basic sites of the

TABLE 5

Physical Properties of Various Catalysts

Catalyst	CeO_2 content /mol%	Number of total basic sites[a] /μ molg^{-1}	Number of weak basic sites[b] /μ molg^{-1}	Specific surface area /m^{2}g^{-1}	Density of weak basic sites[b] /μ mol m^{-2}
MgO[c]	0	1075	177	96	1.8
CeO_2-MgO[c]	1.8	850	180	102	1.8
CeO_2-MgO[c]	3.8	1036	181	108	1.8
CeO_2-MgO[c]	11.2	1202	205	118	1.7
CeO_2-MgO[c]	22.3	1100	154	99	1.6
CeO_2-MgO[c]	40.2	471	75	48	1.6
CeO_2-MgO[c]	72.1	172	46	24	1.9
CeO_2[c]	100	115	115	44	2.6
CeO_2[d]	100	150	150	71	2.1
CeO_2[e]	100	135	135	59	2.3
CeO_2[f]	100	72	72	31	2.3
CeO_2-MgO[g]	1.8	637	171	64	2.7
CeO_2-MgO[g]	3.8	401	90	46	2.0
CeO_2-MgO[g]	11.2	283	53	37	1.4

[a] Total amount of CO_2 desorbed from the sample in the TPD spectra.
[b] Amount of CO_2 desorption peak at lower than 150°C.
[c] Prepared by this method.
[d] Prepared by thermal decomposition of $Ce(NO_3)_3 \cdot 6H_2O$.
[e] Prepared by thermal decomposition of $Ce_2(CO_3)_3 \cdot 8H_2O$.
[f] Prepared by thermal decomposition of $Ce_2(C_2O_4)_3 \cdot 9H_2O$.
[g] Prepared by impregnation.

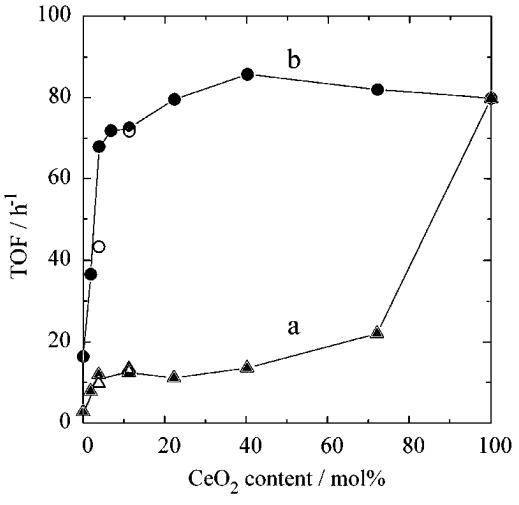

FIG. 8. Variations in the TOF values with CeO_2 content: (a) TOF per a basic site (TOF_t); (b) TOF per a weak basic site (TOF_w). Closed symbols are for the catalysts prepared by this method; open ones for impregnation.

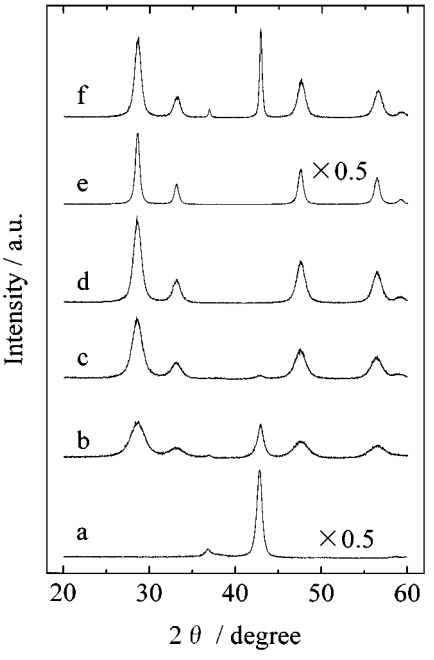

FIG. 9. XRD profiles of CeO_2-MgO catalysts. (a) MgO; (b) CeO_2 (11.2 mol%)-MgO; (c) CeO_2(40.2 mol%)-MgO; (d) CeO_2(72.1 mol%)-MgO; (e) CeO_2 prepared by this method; (f) CeO_2(11.2 mol%)-MgO prepared by impregnation.

samples decreased with increasing CeO_2 content (data not shown).

Thus, we calculated two sets of turnover frequency (TOF) by dividing the reaction rate at 450°C (Table 3) by the total, as well as by the weak basic sites (Table 5). Figure 8 exhibits the variations in the two series of TOF with CeO_2 content, and the values of TOF are summarized in Table 6. The TOF based on the total basic sites (TOF_t) increased with increasing CeO_2 content (curve a). The variation in the TOF_t is similar to that of the reaction rate per unit surface area shown in Table 6. On the other hand, the TOF based on the weak basic sites (TOF_w) of the pure MgO was a fifth of that of the pure CeO_2, and an addition of only 1.8 mol% CeO_2 into MgO increased the TOF_w value (curve b). The TOF_w values of CeO_2-MgO were almost constant at CeO_2 content higher than 6.7 mol% regardless of the preparation methods, and they were equal to that of the pure CeO_2.

TABLE 6

Catalytic Properties of Various Catalysts

Catalyst	CeO_2 content /mol% (wt.%)	Reaction rate[a] /mmol$h^{-1}m^{-2}$	TOF_t[b] /h^{-1}	TOF_w[c] /h^{-1}
MgO[d]	0	0.03	3	16
CeO_2-MgO[d]	1.8 (7.3)	0.07	8	37
CeO_2-MgO[d]	3.8 (14.4)	0.11	12	68
CeO_2-MgO[d]	11.2 (35.0)	0.13	12	73
CeO_2-MgO[d]	22.3 (55.1)	0.12	11	79
CeO_2-MgO[d]	40.2 (74.2)	0.13	14	85
CeO_2-MgO[d]	72.1 (91.2)	0.16	22	83
CeO_2[d]	100	0.21	80	80
CeO_2-MgO[e]	3.8 (14.4)	0.09	10	43
CeO_2-MgO[e]	11.2 (35.0)	0.10	13	72

[a] Reaction rate per unit surface area at 450°C.
[b] Turnover frequency per a basic site.
[c] Turnover frequency per a weak basic site.
[d] Prepared by this method.
[e] Prepared by impregnation.

Figure 9 illustrates XRD profiles of the CeO_2-MgO catalysts. In the XRD profiles of the CeO_2-MgO catalysts prepared by this method, individual phases of CeO_2 and MgO were observed without producing new compounds. CeO_2 diffraction peaks were observed at $2\theta = 28.10$, 33.05, 47.52, 56.53, and 59.10 degrees, corresponding to the Miller indices of (111), (200), (220), (311), and (222), respectively. MgO peaks were observed at $2\theta = 36.97$ and 42.95 degrees to the Miller indices of (111) and (200), respectively. In addition, neither the lattice constants of CeO_2 phase nor those of MgO phase in the catalysts were varied with different CeO_2 contents.

Figure 10 shows variations in the relative peak areas of the diffraction of both CeO_2 (111) peak and MgO (200) peak with CeO_2 content in the CeO_2-MgO prepared by this method. The intensity of the MgO peak decreased with the increase in CeO_2 content, while the intensity of the CeO_2 peak increased. The MgO peak disappeared at the CeO_2 content of 72.1 mol%, while the CeO_2 phase was observed even at CeO_2 content as small as 1 mol%.

Figure 11 depicts variations in the integral widths, which were calculated by dividing the peak areas by their heights, of the CeO_2 (111) and the MgO (200) peaks with CeO_2 content. The width of the CeO_2 (111) peak decreased with

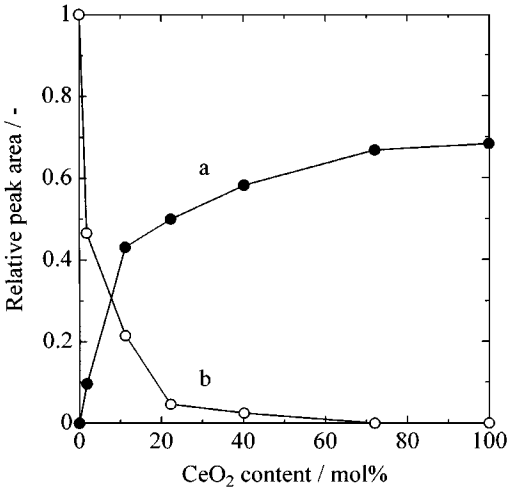

FIG. 10. Variations in the integrated intensities of XRD of CeO_2 and MgO phases in the CeO_2-MgO catalysts with CeO_2 content: (a) CeO_2 (111) face; (b) MgO (200) face.

increasing CeO_2 content while that of the MgO (200) peak was almost constant. A clear difference in the diffraction patterns of the catalysts prepared by different methods was observed in the integral width of the diffraction peaks. In comparison with the diffraction peaks of the CeO_2 (11.2 mol%)-MgO prepared by this method, the widths of the peaks of both MgO and CeO_2 were clearly sharp in the catalyst prepared by impregnation (profile f in Fig. 9): the integral width of the MgO (200) face (0.439 degree) was half of that observed in the pure MgO (0.895 degree), and that of the CeO_2 (111) (1.063 degree) was as sharp as that observed in the pure CeO_2 (0.755 degree).

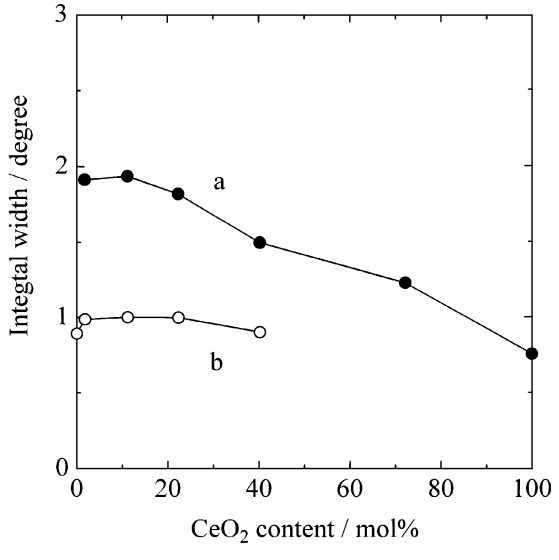

FIG. 11. Variations in the integral widths of diffraction from CeO_2 and MgO with CeO_2 content: (a) CeO_2 (111) face; (b) MgO (200) face.

DISCUSSION

Structure of CeO_2-MgO Catalyst

In the XRD measurement (Fig. 9), each CeO_2-MgO catalyst is found to be a mixture of CeO_2 and MgO regardless of the preparation methods. If the crystal structure of CeO_2 is not strained, the variation in the integral width of the CeO_2 peak is related to the sizes of the CeO_2 particles in the CeO_2-MgO catalyst, according to Scherrer's equation (38), $D_{hkl} = \lambda/\beta \cos\theta$, where D_{hkl}, λ, β, and θ are the volume-averaged particle diameter, the wavelength of the X-radiation, the integral width, and the diffraction angle, respectively. Because the lattice constant of the CeO_2 phase in the catalysts is not varied with CeO_2 content (Figs. 9b–e), the variation in the integral width of the CeO_2 (111) face (Fig. 11a) indicates that the average particle size of CeO_2 increases roughly from 5 to 10 nm with the increase in CeO_2 content. In contrast, the size of the MgO phase in the catalysts is unchanged at a constant size of ca 12 nm because the integral width of MgO (200) face is constant up to the CeO_2 content of 40 mol% (Fig. 11b).

For the CeO_2(11.2 mol%)-MgO catalyst prepared by impregnation (Fig. 9f), the CeO_2 (111) peak which is as sharp as that of the pure CeO_2 is sharper than those observed in the CeO_2-MgO system, and the integral width of the MgO (200) peak is narrower than those observed in the pure MgO and the CeO_2-MgO (Fig. 11). This indicates that large particles of CeO_2 exist on MgO support and that the MgO particles of support grow twice as large as the pure MgO by depositing the dissolved MgO on themselves during the preparation of impregnation. This is a significant difference with the citrate process. Thus, it can be said that citric acid plays a role of dispersing the metal oxide components in the citrate process.

CeO_2 is known to have a fluorite structure such as cubic ZrO_2. In the fluorite structure, cations such as Zr^{4+} and Ce^{4+} are in the closed packing cubic structure, and O^{2-} anions are fully occupied in the tetrahedral sites. Since all of the octahedral sites are vacant, the large vacancy is provided as an interstitial position. Other metal cations are readily substituted in the fluorite structure and, also, inserted in the interstitial positions: Ca^{2+} cations in a cubic ZrO_2 can be located both in the substituted and in the interstitial positions to produce solid solution (39). In the cubic ZrO_2, a change in the lattice constant by substitution is greater than that in the interstitial solid solution. If Ce^{4+} cations were substituted by Mg^{2+} cations in the CeO_2 phase of our system, the lattice constant of the pure CeO_2 should be varied. Judging from the fact that no change in the lattice constant of the CeO_2 phase was observed in our system, it is assumed that Mg^{2+} cations are inserted in the interstitial position of CeO_2 crystallites. The CeO_2 phase probably consists of nonequilibrium solid solution of $Mg_xCe_{1-x/2}O_2$ because of the low calcination temperature of 550°C, although CeO_2

and MgO do not produce a solid solution in the equilibrium state. Actually, in a NiO-MgO system (34), an NaCl-type solid solution is readily obtained in the citrate process even at a low calcination temperature of 550°C. Since the MgO phase in the CeO_2-MgO system disappeared at the CeO_2 content of 72.1 mol% (Fig. 9d), it is speculated that Mg^{2+} cations with at least two-fifths of Ce^{4+} can be inserted in the vacant octahedral sites, forming an interstitial solid solution such as $Mg_{0.4}Ce_{0.8}O_2$.

The specific surface area of the CeO_2(72.1 mol%)-MgO which consists of $Mg_{0.4}Ce_{0.8}O_2$ solid solution is less than that of the pure CeO_2 (Table 5). This means the particle size of the $Mg_{0.4}Ce_{0.8}O_2$ solid solution is larger than that of the pure CeO_2. However, this has a discrepancy with the XRD result that the particle size of CeO_2 calculated from the integral width in the CeO_2(72.1 mol%)-MgO (Fig. 11a) should be smaller than that of the pure CeO_2. Since Mg^{2+} cations inserted in the interstitial positions of CeO_2 do not change the lattice constant of $Mg_{0.4}Ce_{0.8}O_2$, the insertion of Mg^{2+} increases the density of $Mg_{0.4}Ce_{0.8}O_2$. It is speculated that the formation of the solid solution probably decrease the specific surface area of the CeO_2(72.1 mol%)-MgO because of its high density, although it decreases the particle size of the $Mg_{0.4}Ce_{0.8}O_2$ solid solution. In contrast to the high CeO_2-content sample, the specific surface areas of the CeO_2-MgO with low CeO_2 content are much larger than that of the pure CeO_2 (Table 5), because the MgO phase has moderate specific surface areas. Furthermore, since the CeO_2 phase is observed even at CeO_2 content as small as 1 mol%, small CeO_2 particles which consist of solid solution are suggested to be dispersed in the MgO phase. It is elucidated that the active CeO_2-MgO catalyst, for example at the CeO_2 content of 11.2 mol%, consists of the interstitial solid solution of fluorite-type $Mg_xCe_{1-x/2}O_2$ dispersed in the MgO matrix.

Relation between Basic Sites and Catalytic Activities

The TPD detector utilizing an electric conductivity cell immersed in a diluted sodium hydroxide solution is responsive to acidic molecules such as phenol and CO_2, but not to neutral molecules such as methanol and anisole (35, 36). In the TPD spectra of adsorbates on the catalysts used for the methylation at 500°C, most of the adsorbed substrates are desorbed from the CeO_2(11.2 mol%)-MgO (Fig. 5b) and the pure CeO_2 (Fig. 5c) at temperatures lower than 500°C. The signals whose peak tops are around 300°C are probably caused by CO_2 because the used samples are stored in the atmosphere. The substrates adsorbed on the MgO used for the methylation (Fig. 5a), however, are assumed to be phenol and other acidic products because CO_2 is desorbed at lower temperatures (Fig. 6a). The TPD results clearly indicate that acidic substrates are strongly adsorbed on the surface of the pure MgO. It can be also said that the reactant phenol and acidic products readily desorb from the basic sites of CeO_2-MgO and CeO_2 at reaction temperatures higher than 450°C. Actually, the catalytic activity of MgO was deactivated with process time even at 550°C because of the strong adsorption of acidic products.

It is reported that the addition of alkaline metals into MgO enhances the strength of basic sites of MgO (40, 41). Because the addition of alkaline metals into MgO is ineffective to improve the catalytic activities (Table 1), strong basic sites are suggested to be inactive for the methylation of phenol. Owing to the strong adsorption, the strong basic sites cannot release the acidic products at the reaction temperature of 500°C. When we calculated the TOF_t value by dividing the reaction rate by the number of total basic sites, the TOF_t value does not have a clear correlation with CeO_2 content: the TOF_t value gradually increased with increasing CeO_2 content (Fig. 8a). This indicates that the addition of MgO into CeO_2 decreases the methylation ability of the CeO_2 and that total basic sites including strong basic sites are irrelevant to the methylation of phenol at temperatures lower than 500°C.

The properties of several CeO_2 samples prepared by thermal decomposition of cerium salts (4) are added in Table 5. In the series of CeO_2, each CeO_2 has only weak basic sites whose amount is correlated to the specific surface area, and the order of the number of weak basic sites corresponds with the order of the catalytic performance (Table 3). Actually, only weak basic sites were the CeO_2 samples which were effective for the ortho-selective methylation (Table 5).

The deconvolution results in the TPD experiment indicate that the basic sites of MgO consist of at least four different strengths of basic sites and that the CeO_2-MgO also have at least four different strengths of basic sites, as shown in the example of MgO (Fig. 7). In contrast, CeO_2 is proved to have weak basic sites of uniform strength.

In the CeO_2-MgO system, the variation in the weak basic sites with CeO_2 content (the fourth column of Table 5) resembles the variation in the reaction rate (the last column of Table 3). In contrast to the TOF_t (Fig. 8a), the TOF_w, values calculated by dividing the reaction rate by the number of weak basic sites, are almost constant at CeO_2 content higher than 6.7 mol% regardless of the preparation methods (Fig. 8b). It is indicated that the methylation proceeds on the weak basic sites which probably act as adsorption sites of phenol and that the effective weak basic sites are provided on the interstitial solid solution of fluorite-type $Mg_xCe_{1-x/2}O_2$ dispersed in the MgO matrix. It is reported that the ortho position of the phenol perpendicularly adsorbed on a basic site faces the surface of MgO on which the ortho-selective methylation proceeds (42). Since the ortho position of the phenol perpendicularly adsorbed on the weak basic site faces the surface of the CeO_2-MgO catalyst, the ortho-selective methylation probably proceeds at temperatures lower than that on the pure MgO.

Nature of Active Center

Various catalysts reported in the literature are divided into three groups with respect to the reaction temperatures at which the catalyst acts efficiently. Acidic catalysts such as Al_2O_3 (6–8), HY (6, 7, 10), H-ZSM5 (6, 7, 9, 10), and Nafion-H (8, 43) have their methylation activities at temperatures lower than 300°C, whereas they are less selective because of their catalysis for both oxygen-methylation and ring-methylation. Various mixed oxides (1, 3, 11–21) show their catalytic activities at the temperature range between 300 and 450°C, and they are selective to the ortho-methylation of phenol. Furthermore, simple oxides such as MgO (1–4), CeO_2 (4), Mn_3O_4 (5), and ThO_2 (44) show their catalytic activities at temperatures higher than 450°C, and most of them are more selective to the ortho-position. By way of exception, ThO_2 (44) catalyzes the oxygen-alkylation to produce selectively anisole at 500°C. Because the desorption process of acidic products, as well as the activation of methanol, is important in the catalytic reaction, acid–base properties of catalysts are assumed to be a major factor of determining the optimum reaction temperature.

In the methylation of phenol over an acidic alumina, the anisole formation is preferential at temperatures as low as 200°C, and ring-methylated products are dominant at elevated temperatures as 300°C (8, 45). Anisole is converted into *o*-cresol and other methylated phenols over acidic catalysts, and anisole also acts as a methylating reagent to produce methylanisole (8, 19, 20). As shown in Table 4, both the CeO_2-MgO and the pure CeO2 do not have any activity for the transformation of anisole into *o*-cresol in the catalytic conversion of anisole at 500°C. Therefore, they have no acidic sites which catalyze the methyl migration of anisole, and they catalyze only the direct alkylation of phenol with methanol.

Because neither dimethyl ether formation in the methylation nor ammonia adsorption in the TPD experiment is observed, no acidic sites are concluded to be on the CeO_2-MgO catalysts. Although an acid–base pair site has been proposed as an active center for the alkylation over alumina (8), a methyl cation produced on nonacidic sites should not be speculated to attack the ortho-positions of phenol perpendicularly adsorbed on the weak basic sites in our system. If the basic sites activate methanol, methoxy anion can be produced. However, we should not assume that methoxy anion reacts with electron-rich phenol molecules adsorbed on weak basic sites, either.

In the methanol decomposition without phenol, methanol is found to be decomposed into CO and CH_4 even at the reaction temperature as low as 450°C over the pure CeO_2 and the CeO_2-MgO catalysts (Table 2). Although the density of weak basic sites of the pure MgO is similar to those measured in the CeO_2-MgO samples (Table 5), the pure MgO is less active than the CeO_2-MgO and nonselective to CH_4 in the methanol decomposition. This indicates that the activation of methanol is also significant for the catalytic methylation and that the CeO_2-containing catalysts have the activation of methanol, such as the dehydrogenation of methanol and the hydrogenation of CO. Actually, CeO_2 itself is known to have the ability of the hydrogenation of CO (46). In the methylation of phenol, we speculate that the redox property of the CeO_2 species is concerned with methanol activation, and methanol is activated on the CeO_2 species as a form of formyl or hydroxy methyl group rather than methyl cation on acidic sites. Although formaldehyde may be used as a methylating reagent, we do not examine the methylation of phenol with formaldehyde instead of methanol.

No change in the TOF_w is observed at CeO_2 content higher than 6.7 mol% (Fig. 8b), and the catalytic behavior in the methanol decomposition is quite similar between the pure CeO_2 and the CeO_2(11.2mol%)-MgO (Table 2). These results also indicate that the formation of solid solution such as $Mg_{0.4}Ce_{0.8}O_2$, which is discussed above, does not influence the catalytic properties of the CeO2 phase, and that the excess MgO in the CeO_2-MgO catalyst acts as a support for the solid solution of $Mg_xCe_{1-x/2}O_2$.

Different Catalytic Activities in the System

Temperature dependence in the catalytic behaviors is different from each other among MgO (Fig. 2), CeO_2-MgO (Fig. 3), and CeO_2 (Fig. 4). In all the catalysts we tested, only the pure CeO_2 and the CeO_2-MgO exhibit no activity decay in the methylation. Although the matrix of MgO in the CeO_2-MgO catalyst is essentially MgO (Figs. 9b–d), the activity decay behaviors of MgO (Figs. 2a–c) disappear in the CeO_2-MgO system (Figs. 3a–c). Because the conversion level of the pure MgO is lower than that of the pure CeO_2 (Figs. 1a–c), the decay behaviors of MgO are suggested to be hidden in the stable high catalytic performance of the CeO_2-MgO. Similarly, in the series of MgO-based mixed oxides, except for Ce and U (Table 1), the MgO matrix is said to be a major catalyst source, whereas the second components do not effectively work as catalysts.

The difference in the temperature dependence in the catalytic behaviors can be discussed in connection with the results of Fig. 5. The basic strength of CeO_2 is weak enough to desorb the products from its surface at temperatures between 450 and 550°C, while that of MgO is too strong to desorb the products and the reactant. The phenol conversion of pure MgO, however, greatly increases at the reaction temperature between 500 and 550°C (Figs. 2b and c). Much stronger basic sites of the pure MgO possibly release the acidic products at the higher temperature of 550°C. In addition, the phenol conversion slightly increases between 500 and 550°C over CeO_2-MgO (Fig. 3). This indicates that basic sites of medium strength which are attributed to the MgO phase in the CeO_2-MgO samples

become effective to release the products at temperatures as high as 550°C. In contrast, the phenol conversion passes through a maximum at 500°C over the pure CeO_2 (Fig. 4), because methanol decomposes at 550°C.

At the methylation temperature of 600°C, however, the catalysts are steeply deactivated, and coke formation is observed. The methanol decomposition without phenol is not deactivated at 600°C regardless of the basic strength of the catalysts. Thus, the deactivation in the methylation at 600°C is said to be attributed to the polymerization of phenol followed by coking.

CONCLUSION

Selective ortho-methylation of phenol with methanol was performed over CeO_2-MgO catalysts prepared using a molten mixture of cerium (III) nitrate, magnesium nitrate, and citric acid. The CeO_2-MgO was found to have attractive catalytic performance without decay of activities and had excellent selectivities to the sum of *o*-cresol and 2,6-xylenol higher than 98% at a temperature range between 450 and 550°C. The pure CeO_2 exhibited an efficient ortho-selectivity and the optimum activity in the methylation at 500°C, whereas the pure MgO showed the optimum activity at 550°C with a decay in the catalytic activity. This is concerned with the strength of basic sites of catalyst; the pure CeO_2 had only weak basic sites in contrast to strong basicity of the pure MgO.

In the XRD measurement, the CeO_2-MgO catalyst was a mixture of MgO and an interstitial solid solution of CeO_2 with MgO. It is confirmed that citric acid used in the preparation heightens the dispersion of the interstitial solid solution of $Mg_xCe_{1-x/2}O_2$ in the MgO matrix. In the results of methanol decomposition without phenol, methanol was decomposed into CO, CO_2, and CH_4 over the CeO_2-MgO catalysts, without forming dimethyl ether.

The turnover frequency based on the weak basic sites is constant at CeO_2 content higher than 6.7 mol% regardless of preparation methods. The reaction mechanism of the ortho-methylation over CeO_2-MgO catalyst is speculated: the ortho position of phenol adsorbed perpendicularly on a weak basic site on CeO_2 species is selectively alkylated by methanol which is possibly activated in the form of formyl or hydroxy methyl group rather than methyl cation.

REFERENCES

1. Fukuda, Y., Nishizaki, T., and Tanabe, K., *Nihon Kagaku Kaishi*, 1754 (1972).
2. Nozaki, F., and Kimura, I., *Bull. Chem. Soc. Jpn.* **50**, 614 (1977).
3. Tanabe, K., Hattori, H., Sumiyoshi, T., Tamaru, K., and Kondo, T., *J. Catal.* **53**, 1 (1978).
4. Sato, S., Koizumi, K., and Nozaki, F., *Appl. Catal. A* **133**, L7 (1995).
5. Bezouhanova, C., and Al-Zihari, M. A., *Appl. Catal.* **83**, 45 (1992).
6. Pierantozzi, R., and Nordquist, A. F., *Appl. Catal.* **21**, 263 (1986).
7. Belitrame, P., Belitrame, P. L., Carniti, P., Castelli, A., and Forni, L., *Appl. Catal.* **29**, 327 (1987).
8. Santacesaria, E., Grasso, D., Gelosa, D., and Carra, S., *Appl. Catal.* **64**, 83 (1990).
9. Santacesaria, E., Diserio, M., Ciambelli, P., Gelosa, D., and Carra, S., *Appl. Catal.* **64**, 101 (1990).
10. Balsama, S., Beltrame, P., Beltrame, P. L., Carniti, P., Forni, L., and Zuretti, G., *Appl. Catal.* **13**, 161 (1984).
11. Kotanigawa, T., Yamamoto, M., Shimokawa, K., and Yoshida, Y., *Bull. Chem. Soc. Jpn.* **44**, 1961 (1971).
12. Kotanigawa, T., and Shimokawa, K., *Bull. Chem. Soc. Jpn.* **47**, 950 (1974).
13. Kotanigawa, T., and Shimokawa, K., *Bull. Chem. Soc. Jpn.* **47**, 1535 (1974).
14. Grabowska, H., Kaczmarczyk, W., and Wrzyszcz, J., *Appl. Catal.* **47**, 351 (1989).
15. Misono, M., and Nojiri, N., *Appl. Catal.* **64**, 1 (1990).
16. Narayanan, S., Venkatrao, V., and Durgakumari, V., *J. Mol. Catal.* **52**, L29 (1989).
17. Venkatrao, V., Durgakumari, V., and Narayanan, S., *Appl. Catal.* **49**, 165 (1989).
18. Venkatrao, V., Chary, K. V. R., Durgakumari, V., and Narayanan, S., *Appl. Catal.* **61**, 89 (1990).
19. Velu, S., and Swamy, C. S., *Appl. Catal. A* **119**, 241 (1994).
20. Velu, S., and Swamy, C. S., *Appl. Catal. A* **145**, 141 (1996).
21. Velu, S., and Swamy, C. S., *Appl. Catal. A* **145**, 225 (1996).
22. Marcilly, C., Courty, P., and Delmon, B., *J. Am. Ceram. Soc.* **53**, 56 (1970).
23. Zhang, H. M., Teraoka, Y., and Yamazoe, N., *Chem. Lett.*, 665 (1987).
24. Ramos, I. R., Ruiz, A. G., Rojas, M. L., and Fierro, J. L. G., *Appl. Catal.* **68**, 217 (1991).
25. Forni, L., Oliva, C., Vishniakov, A. V., Ezerets, A. M., Mukovozov, I. E., Vatti, F. P., and Zubkovskaja, V. N., *J. Catal.* **145**, 194 (1994).
26. Slagtern, A., and Olsbye, U., *Appl. Catal. A* **110**, 99 (1994).
27. Courty, P., Durand, D., Freund, E., and Sugier, A., *J. Mol. Catal.* **17**, 241 (1982).
28. Cosimo, J. I. D., Marchi, A. J., and Apesteguia, C. R., *J. Catal.* **134**, 594 (1992).
29. Kim, K. M., Woo, H. C., Cheong, M., Kim, J. C., Lee, K. H., Lee, J. S., and Kim, Y. G., *Appl. Catal. A* **83**, 15 (1992).
30. Sato, S., Iijima, M., Nakayama, T., Sodesawa, T., and Nozaki, F., *J. Catal.* **169**, 447 (1997).
31. Nakayama, T., Sato, S., and Nozaki, F., *Bull. Chem. Soc. Jpn.* **69**, 2107 (1996).
32. Sato, S., Nozaki, F., and Nakayama, T., *Appl. Catal. A* **139**, L1 (1996).
33. Nakayama, T., Sato, S., Yamashiro, K., and Nozaki, F., *Appl. Catal. A* **151**, 437 (1997).
34. Nakayama, T., Ichikuni, N., Sato, S., and Nozaki, F., *Appl. Catal. A* **158**, 185 (1997).
35. Sato, S., Tokumitsu, M., Sodesawa, T., and Nozaki, F., *Bull. Chem. Soc. Jpn.* **64**, 1005 (1991).
36. Sato, S., Takematsu, K., Sodesawa, T., and Nozaki, F., *Bull. Chem. Soc. Jpn.* **65**, 1486 (1992).
37. Sato, S., Kuroki, M., Sodesawa, T., Nozaki, F., and Maciel, G. E., *J. Mol. Catal. A* **104**, 171 (1995).
38. Scherrer, P., *Goetinger Nachr.* **2**, 98 (1918).
39. Diness, R., and Roy, R., *Solid State Comm.* **3**, 123 (1965).
40. Matsuda, T., Sasaki, Y., Miura, H., and Sugiyama, K., *Bull. Chem. Soc. Jpn.* **58**, 1041 (1985).
41. Kanno, K., and Kobayashi, M., *Bull. Chem. Soc. Jpn.* **66**, 3806 (1993).
42. Tanabe, K., and Nishizaki, T., *in* "Proc. 6th Int. Congr. Catal., 1976," Vol. 2, p. 863. Chem. Soc., London, 1977.
43. Kaspi, J., and Olah, G. A., *J. Org. Chem.* **43**, 3142 (1978).
44. Karuppannasamy, S., Narayanan, K., and Pillai, C. N., *J. Catal.* **66**, 281 (1980).
45. Samolada, M. C., Grigoriadou, E., Kiparissides, Z., and Vasalos, I. A., *J. Catal.* **152**, 52 (1995).
46. Li, C., Domen, K., Maruya, K., and Onishi, T., *J. Catal.* **141**, 540 (1993).